Radiative recombination into high-Z few-electron ions: Cross sections and angular distributions

Stephan Fritzsche* and Andrey Surzhykov†
Institut für Physik, Universität Kassel, D-34132 Kassel, Germany

Thomas Stöhlker
Gesellschaft für Schwerionenforschung (GSI), D-64291 Darmstadt, Germany and Institut für Kernphysik, Universität Frankfurt, D-60486 Frankfurt, Germany
(Received 3 March 2005; published 5 July 2005)

The radiative electron capture into high-Z, few-electron ions is studies in the framework of the density matrix, based on Dirac's equation. In this formalism, all the properties of the photons and the (remaining) ions can be described, independent from their initial shell structure or polarization. Detailed computations have first been carried out for the total and angle-differential cross sections, following the capture of an electron into hydrogen-U^{91+} and lithiumlike U^{89+} ions. From these calculations, which were performed in two different approximations, it is shown that many-electron interactions affect the angular distribution at low projectile energies by about 5%. Apart from describing the (angular-dependent) capture cross sections, our formalism is also appropriate to explore the subsequent $K\alpha,\beta$ photon emission, if the electron is captured into an excited state of the ion, the polarization of the photons and ions as well as the interplay of the radiative with other, nonradiative capture processes in the future.

DOI: 10.1103/PhysRevA.72.012704 PACS number(s): 34.70.+e, 31.25.−v, 31.30.Jv

I. INTRODUCTION

At storage rings, the radiative capture of electrons by fast high-Z projectiles is one of the dominant interaction process which cause a loss of ions from the beam. In this recombination process, a (quasi) free electron from either the (electron) cooler or some rest gas is captured into a bound state of the ion under the simultaneous emission of a photon. In fact, the radiative recombination (RR) of ions, known also as the radiative electron capture (REC) of loosely bound electrons, is the time-reversed photoionization and a process, which frequently occurs in (almost) all types of plasmas.

Because of their practical importance, detailed REC studies have been carried out in the past for many elements and for a wide range of projectiles energies (up to several hundred MeV/u). In the high-Z domain, however, the main attention was paid so far to the capture into bare ions [1–4], leading to hydrogenlike ions after the recombination has taken place. Apart from the total and angle-differential cross sections, these investigations provided valuable information about the electron-photon interaction in the presence of strong fields. In the theoretical description of this process, the use of the density matrix in particular helped to reveal many details about the capture process, including the angular distribution and polarization of the subsequent Lyman-$\alpha_{1,2}$ decay [5–7], if the electron was captured into an excited state of the ion, as well as the polarization of the emitted REC photons [8,9], in excellent agreement with experiment. Recently, moreover, the application of the density matrix formalism allowed us to analyze the REC photon emission in dependence of the polarization of the incident particles [10,11] which, in the future, might become a tool for determining the polarization of ion beams at storage rings. Apart from the REC into bare ions, however, less emphasis was placed on the capture into high-Z few-electron ions, partially also because no (many-electron) computations are available for heavy open-shell ions. In two earlier experiments [12,13], for example, only the total K- and L-shell cross sections for the capture into H-, He-, and Li-like uranium were measured and compared with scaled one-electron calculations. For the capture into He-like (i.e., closed-shell) ions with kinetic energy 10 MeV/$u \leqslant T_p \leqslant 700$ MeV/u, in addition, the electron-electron correlation was explored also in the framework of quantum electrodynamics [14] but was found of minor importance ($\lesssim 2\%$) for the total REC cross sections.

In this contribution, we extend the density matrix formalism to deal with the capture into high-Z few-electron ions, independent of the shell structure of the ions in their initial and final states. Although this formalism will first be applied (below) only to the total and the angle-differential REC cross sections, the theory is appropriate for instance (and has been derived here up to statistical tensors of the remaining ion) for studying the subsequent decay of the ions, if possible, or the effects of either the ion or electron polarization onto the recombination of the ions. In Sec. II, we present the density matrix formalism for the capture into many-electron ions and show how the computation of (most) REC properties can be traced back to the definition of a reduced matrix element (transition amplitude) which couples the bound-state density of the remaining ion to the one-electron continuum. In Sec. III, these matrix elements are then calculated in the framework of the multiconfiguration Dirac-Fock (MCDF) method. In particular, detailed computation have been carried out for the capture into hydrogen- and lithium-like uranium ions. The total and angle-differential cross sections obtained are discussed in Sec. IV as function of the projectile energy and are compared to results from an independent particle model,

*Electronic address: s.fritzsche@physik.uni-kassel.de
†Electronic address: surz@physik.uni-kassel.de

based on hydrogenic functions. These computations demonstrate that many-electron effects become important not only for the capture into the L and M shells, but also at low energies of the projectiles. Even larger effects are expected if such a many-electron theory is applied for studying the polarization of the emitted x-ray photons as the spin state of the photons is known to be sensitive to electron-electron correlations. Finally, a brief summary and outlook is given in Sec. V.

II. THEORY

A. Radiative electron capture

In (fast) electron-ion collisions, the angular distribution and polarization properties of the particles involved are best described within the framework of the density matrix theory [15,16]. In the past few years, for instance, this theory helped to analyze a number of measurements where electrons were captured by bare high-Z ions [10]. Here, we now extend the theory to the capture of electrons by few-electron ions, for which the use of the density matrix is expected to be even more useful since it enables one to take into account also the internal structure of the ions. In fact, there are several features of the density matrix theory which we shall consider in going from bare ions to (the electron capture into) few- and many-electron systems. In addition to the need of a proper notation for the density matrix (elements) of the overall collision system, we wish to prepare the formalism general enough in order to allow for a nonzero nuclear spin as required, for example, for describing the effects of the ion polarization on the capture of electrons. Such a generalization of the theory is necessary, moreover, if the electrons are captured into an excited state and if one wishes to understand the subsequent photon emission.

Therefore, in order to derive the theory in sufficient general form, let us start from the notation of the initial and final states of the overall system. For the capture of a single electron, the initial state is given by the ion "plus" the free electron. For most experiments, here we may consider (in very good approximation) an electron with well-defined asymptotic momentum $\mathbf{p}$ and spin projection m_s. This approximation is appropriate even for the capture of a quasi-free-electron as it occurs in the collision of heavy ions with light target atoms [1]; in fact, the use of the momentum $\mathbf{p}$ and the spin projection m_s is the most general form in order to describe the dynamical and polarization properties of the electron. The ion, in contrast, is initially supposed in a state $|\alpha_i J_i M_{J,i}\rangle$ with well-defined total angular momentum J_i, $M_{J,i}$ (of the electrons), and where α_i is used to denote all additional quantum numbers as required for a unique specification of the states.

The notation above for the initial state of the ion is appropriate, of course, only for a zero nuclear spin $I=0$. For a nonzero spin $I>0$, instead, the ion will be found in a hyperfine state $|(I,\alpha_i J_i)F_i M_{F,i}\rangle$ (or some mixture of such states), where $\mathbf{F}=\mathbf{I}+\mathbf{J}$ is the total angular momentum and $M_{F,i}$ the corresponding spin projection. In this section, we shall include the nuclear spin in our notation from the very beginning in order to "prepare" a (forthcoming) analysis of the photon emission in dependence of the nuclear spin as well as the hyperfine structure and the polarization of the ions in their initial state. For calculating the total and angle-differential REC cross sections, in contrast, it will be sufficient later to set $I=0$ in all formulas, at least as long as the hyperfine interaction (between the magnetic moments of the electrons and nuclei) is omitted from the computations.

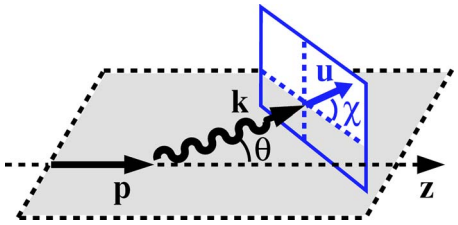

FIG. 1. (Color online) The unit vector $\mathbf{u}(\chi)$ of the linear polarization is defined in the plane, which perpendicular to the photon momentum $\mathbf{k}$, and is characterized by an angle χ with respect to the reaction plane.

Following the capture of an electron, the final-state of the overall system is given by the recombined ion in some (final) state $|(I,\alpha_f J_f)F_f M_{F,f}\rangle$ and the recombination photon with wave vector $\mathbf{k}$ and polarization vector $\mathbf{u}$. The vector $\mathbf{u}$, of course, can be written always in terms of any two (linear-independent) basis vectors which are perpendicular to $\mathbf{k}$, such as $\mathbf{u}_{+1}$ and $\mathbf{u}_{-1}$ for right- and left-polarized photons [16], respectively. Still, the notation of the collision system is not yet complete as the choice of the coordinates and, hence, the projection of the quantum states also depend on the geometry in which an experiment is carried out. To describe the radiative capture of electrons both, the direction of the incoming electron and that of the emitted photons can be chosen for quantization (see Fig. 1) and have been discussed recently [8]. While the photon direction is (usually) convenient for analyzing the total and angle-differential REC cross sections (at least from a computational viewpoint), the direction of the electron momentum is more general, in particular, if the polarization of either the ions of photons are to be considered. At storage rings, moreover, the electron momentum also coincides with the direction of the ion beam in the experiment.

B. Density matrix formalism

In the (time-independent) density matrix theory, the state of a physical system is characterized by means of statistical operators which describe a single or an ensemble of equally prepared collision systems in either a *pure* quantum state or in a *mixture* of different states with any degree of coherence [15,16]. The great benefit of the density matrix theory is that it virtually allows to "accompany" such an ensemble through the collision process without that the quantum-mechanical information is getting lost. Starting from a well-defined initial state of the collision system, in fact, one may follow up the system through one or several regions of interaction until the final state of the collision and/or the decay process is attained. A physical characterization of the process is then achieved by making use of a proper set of detector operators

which "measure" (some or all of) the particles as involved in the collision.

With the notation above for the capture of an electron into a bound state of the ion, the initial state density matrix of the combined system "ion+electron" is given by

$$\hat{\rho}_i = \hat{\rho}_i^{\text{ion}} \otimes \hat{\rho}_e, \tag{1}$$

i.e., the tensor product of the density matrices of the two subsystems. If neither the electrons nor the ions are polarized initially, the tensor product can be written as

$$\hat{\rho}_i = \frac{1}{2(2F_i+1)} \sum_{m_s M_{F,i}} |(I,\alpha_i J_i)F_i M_{F,i}\rangle|\mathbf{p}m_s\rangle\langle\mathbf{p}m_s| \times\langle(I,\alpha_i J_i)F_i M_{F,i}| \tag{2}$$

including the coupling of the nuclear spin I. From this initial-state matrix, the final-state density matrix $\hat{\rho}_f$ is obtained from the standard relation

$$\hat{\rho}_f = \hat{\mathcal{R}}^\dagger \hat{\rho}_i \hat{\mathcal{R}}, \tag{3}$$

where $\hat{\mathcal{R}}$ is called the transition operator and describes the interaction of the electrons with the radiation field. For a more detailed representation of this operator, of course, we first need to consider the coupling of the free electron to the bound-state electron density in the initial state of the system as well as the decomposition of the photon field within the relativistic theory. Moreover, since we wish to consider the electron capture by high-Z ions, any thorough description of the electron-photon interaction should be based on Dirac's equation and the *minimal coupling* of the radiation field. Note that a relation analog to Eq. (3) can be used in order to refer to any subsequent excitation or decay of the ion following the REC process. For the present study of the total and angle-differential cross sections, however, it is sufficient to restrict the approach to just a single interaction.

Equation (3) describe the final-state density operator and, thus, contains all the information about the system following the capture of an electron and the (simultaneous) emission of the photon with wave vector $\mathbf{k}=(k,\theta,\varphi)$. Instead of using the final-state density operator $\hat{\rho}_f$, however, it is often more convenient to work with a matrix representation of the operator, briefly referred to as the final-state density matrix. In a basis with well-defined (angular) momenta, the final-state density matrix is given by

$$\begin{aligned}\langle(I,\alpha_f J_f)F_f M_{F,f},\mathbf{k}\lambda|\hat{\rho}_f|(I,\alpha_f J_f)F_f M'_{F,f},\mathbf{k}\lambda'\rangle &= \frac{1}{2(2F_i+1)} \sum_{M_{F,i}m_s} \langle(I,\alpha_f J_f)F_f M_{F,f},\mathbf{k}\lambda|\hat{\mathcal{R}}^\dagger|(I,\alpha_i J_i) \\ &\times F_i M_{F,i},\mathbf{p}m_s\rangle\langle(I,\alpha_i J_i)F_i M_{F,i},\mathbf{p}m_s|\hat{\mathcal{R}}|(I,\alpha_f J_f) \\ &\times F_f M'_{F,f},\mathbf{k}\lambda'\rangle,\end{aligned} \tag{4}$$

if we assume that both the incident electrons and ions are initially unpolarized [see Eq. (2)]. Obviously, the information about the radiative capture is now contained in the transition matrix $\langle(I,\alpha_i J_i)F_i M_{F,i},\mathbf{p}m_s|\hat{\mathcal{R}}|(I,\alpha_f J_f)F_f M_{F,f},\mathbf{k}\lambda\rangle$ which we shall evaluate further in Sec. II E below. To extract the observable properties from the density matrix (4), however, we need to specify also the "detector operator" due to the actual setup of the detectors in the given experiment. Broadly speaking, the detector operator *projects out* all those quantum states which lead to a "click" at the detector. In the density matrix theory, the detector operator $\hat{P}$ determines the probability for an "event" at the detectors simply by taking the trace of its product with the density matrix $W=\text{Tr}(\hat{P}\hat{\rho}_f)$. To measure, for instance, the angular distribution of the recombination photons in the direction $\hat{\mathbf{n}}=(\theta,\varphi)$ with a detector, which is sensitive to the energies but not to the polarization of the photons, the detector operator is

$$\hat{P}_{\mathbf{k}} = \sum_{\lambda M_{F,f}} |\mathbf{k}\lambda\rangle|(I,\alpha_f J_f)F_f M_{F,f}\rangle\langle(I,\alpha_f J_f)F_f M_{F,f}|\langle\mathbf{k}\lambda|. \tag{5}$$

Taking the trace over the product of this operator with the density matrix (4), $\text{Tr}(\hat{P}_{\mathbf{k}}\hat{\rho}_f)$, we immediatly obtain the angle-differential cross section

$$\frac{d\sigma^{\text{REC}}_{|F\rangle}}{d\Omega}(\theta,\phi) = \sum_{\lambda M_{F,f}} \langle(I,\alpha_f J_f)F_f M_{F,f},\mathbf{k}\lambda|\hat{\rho}_f|(I,\alpha_f J_f)F_f M_{F,f},\mathbf{k}\lambda\rangle \tag{6}$$

which, for unpolarized electrons and ions, can be cast into the (familiar) form

$$\frac{d\sigma^{\text{REC}}_{|F\rangle}}{d\Omega}(\theta,\phi) = \frac{1}{2(2F_i+1)} \sum_{\lambda,M_{F,f},m_s,M_{F,i}} |\langle(I,\alpha_i J_i) F_i M_{F,i},\mathbf{p}m_s|\hat{\mathcal{R}}|(I,\alpha_f J_f)F_f M_{F,f},\mathbf{k}\lambda\rangle|^2, \tag{7}$$

including a summation over all magnetic quantum numbers λ, $M_{F,f}$, m_s, $M_{F,i}$ of the initial and final subsystems of the REC process. Below, we will further simplify formula (7) for the angle-differential cross sections by applying a spherical-tensor representation of the electron-photon interaction and the techniques from Racah's algebra. From the differential cross sections, the total cross sections are obtained as

$$\begin{aligned}\sigma^{\text{REC}}_{|F\rangle} &= \int d\Omega \frac{d\sigma^{\text{REC}}_{|F\rangle}}{d\Omega}(\theta,\phi) \\ &= \sum_{\lambda M_{F,f}} \int d\Omega \langle(I,\alpha_f J_f)F_f M_{F,f},\mathbf{k}\lambda|\hat{\rho}_f|(I,\alpha_f J_f)F_f M_{F,f},\mathbf{k}\lambda\rangle,\end{aligned} \tag{8}$$

i.e., by the integration over all 4π solid angles.

Apart from studying the angular distribution of the recombination photons, the final-state density matrix (4) can be used also to separate the density matrices of the individual subsystems and to obtain the (reduced) matrices for the recombination photons and the residual ions. Although no detailed computations have yet been carried out on the reduced density matrices (or those observables which are associated with such a reduction), a few remarks are in place here in order to present the theoretial background for a forthcoming investigation concerning the alignment of the ion in the final state of the REC and its subsequent decay (if possible). Sup-

pose, the emitted REC photons remain unobserved in an experiment, the density matrix of the residual ion

$$\begin{aligned}\langle (I,\alpha_f J_f) F_f M_{F,f} | \hat{\rho}_f^{\rm ion} | (I,\alpha_f J_f) F_f M'_{F,f} \rangle \\ = {\rm Tr}_\gamma(\hat{\rho}_f) \\ = \sum_\lambda \int d\Omega \langle (I,\alpha_f J_f) F_f M_{F,f}, \mathbf{k}\lambda | \hat{\rho}_f | (I,\alpha_f J_f) F_f M_{F,f}, \mathbf{k}\lambda \rangle\end{aligned} \tag{9}$$

is obtained by taking the trace over the (direction and the polarization states of the) photons. From Eq. (8), moreover, we see that the density matrix (9) of the residual ion is normalized in a way that its trace is equal to the total REC cross section

$$\sum_{M_{F,f}} \langle (I,\alpha_f J_f) F_f M_{F,f} | \hat{\rho}_f^{\rm ion} | (I,\alpha_f J_f) F_f M_{F,f} \rangle = \sigma^{\rm REC}_{|F\rangle}, \tag{10}$$

for the capture of an electron into a given (hyperfine) level as appropriate for studying the alignment of the ions. In addition to the reduced density matrix (9), it is sometimes more convenient to represent the final state of the ions in terms of their statistical tensors [5,15]

$$\begin{aligned}\rho_{kq}((I,\alpha_f J_f) F_f) = \sum_{M_{F,f} M'_{F,f}} (-1)^{F_f - M'_{F,f}} \langle F M_{F,f} F - M'_{F,f} | kq \rangle \\ \times \langle (I,\alpha_f J_f) F_f M_{F,f} | \hat{\rho}_f^{\rm ion} | (I,\alpha_f J_f) F_f M'_{F,f} \rangle\end{aligned} \tag{11}$$

which are constructed to transform similar to the spherical harmonics of rank k under a rotation of the coordinates. Although both, the reduced density matrix (9) and the statistical tensors (11) are mathematically equivalent, the latter form enables one to exploit the rotational symmetry of free atoms and ions. In our forthcoming work, therefore, we shall apply these (spherical) statistical tensors in order to analyze the alignment and decay of the residual ions, if the electrons were captured into an excited state.

C. Many-electron bound and scattering states

To evaluate the angular distribution (7) or the statistical tensors (11), we first need to simplify the transition matrix

$$\begin{aligned}\langle (I,\alpha_i J_i) F_i M_{F,i}, \mathbf{p} m_s | \hat{\mathcal{R}} | (I,\alpha_f J_f) F_f M_{F,f}, \mathbf{k}\lambda \rangle \\ = \langle (I,\alpha_i J_i) F_i M_{F,i}, \mathbf{p} m_s | \hat{\mathcal{R}}_\lambda(\mathbf{k}) | (I,\alpha_f J_f) F_f M_{F,f} \rangle\end{aligned} \tag{12}$$

and to bring it into a form which is computationally feasible even within the framework of Dirac's theory. As seen from Eq. (12), there occurs two types of many-electron states on the left-hand side (LHS) and right-hand side (RHS) of the matrix elements which we shall discuss separately below. While, initially, we have a scattering state with one electron in the continuum (LHS), the final state of the ion is given by an ordinary bound state (RHS) [17].

Let us begin with the wave functions for the bound states of the ions for which a large number of methods are known from the theory of atomic structure in order to generate approximate solutions. Since the nucleus is taken to be independent of the electron density, we may use the standard Clebsch-Gordan expansion for the coupling of two angular momenta to decouple the nuclear spin

$$|(I,\alpha J) F M_F\rangle = \sum_{M_I M_J} \langle I M_I J M_J | F M_F \rangle | I M_I \rangle | \alpha J M_J \rangle \tag{13}$$

from the bound-state electrons and to consider just the (many-) electron states $|\alpha J M_J\rangle \equiv |\alpha J P M_J\rangle$ with well-defined total angular momentum J, M_J, and parity P. Together with an analog expansion on the LHS of the matrix elements in Eq. (12), the summation over the (four) magnetic quantum numbers leads to a Wigner 6-j symbol, in line with the recoupling of the three angular momenta of the nucleus as well as the electrons in the (total) initial and final states of the process. Apart from the (N-electron) final state of the ion, of course, the notation $|\alpha J M_J\rangle$ can be used also to refer to the $(N-1)$ bound electrons in the initial state; it implies moreover an antisymmetrization of the wave functions with respect to all (bound-electron) coordinates. In Sec. III, we shall briefly explain the construction of the bound states within the framework of the MCDF method as used below for calculating the total and angle-differential cross sections.

Often, the (stable) bound states of an ion are associated with a well-defined shell structure, i.e., a particular occupation and coupling of the one-electron orbitals, and can thus be approximated rather easily within the atomic shell model. Greater care, in contrast, is required if we wish to construct realistic scattering states with one electron in the continuum as they appear on the LHS of Eq. (12). These scattering states (have to) represent the initial ion with well-defined angular momentum J_i, $M_{J;i}$ as well as a free electron with momentum $\mathbf{p}$ and spin projection m_s, which moves in the field of the ion. For the further evaluation of the matrix elements (12), therefore, it is covenient to start with the decomposition of the free-electron wave into partial waves [1]

$$|\mathbf{p} m_s\rangle = \sum_\kappa i^l e^{i\Delta_\kappa} \sqrt{4\pi} [l]^{1/2} \langle l 0 1/2 m_s | j m_s \rangle | \epsilon\kappa j m_s \rangle, \tag{14}$$

in order to construct those (many-electron) components of the scattering states $|\alpha_i J_i, \mathbf{p} m_s\rangle$, which have a well-defined total angular momentum J, M and parity P. In the expansion (14) of the free-electron wave, the summation runs over Dirac's angular momentum quantum number

$$\kappa \equiv \kappa(j,l) = \pm (j + 1/2) \quad \text{for} \quad l = j \pm 1/2,$$

where j is the total (one-electron) angular momentum, -1^l the parity of the partial waves $|\epsilon\kappa j m_s\rangle$, and $[l] \equiv (2l+1)$. Furthermore, the phase shift Δ_κ arises due to the (non-Coulombic) field of the nucleus and the remaining electrons, and where the + sign indicates the boundary condition for the capture of an electron, i.e., the superposition of a plane wave and an outgoing spherical wave. Each partial wave in Eq. (14) separate, as usual, into a radial and angular part [1,18]

$$\langle r|\epsilon\kappa jm_s\rangle = \frac{1}{r}\begin{pmatrix} P_{\epsilon\kappa}(r)\chi_{\kappa}^{m_s} \\ iQ_{\epsilon\kappa}(r)\chi_{-\kappa}^{m_s}\end{pmatrix}, \tag{15}$$

in which $\chi_{\kappa}^{m_s}$ denotes a standard Dirac spin-angular function, and where the two (radial) functions $P_{E\kappa}(r)$ and $Q_{E\kappa}(r)$ are often called the large and small components, respectively. In the evaluation of the transition matrix (12), of course, the radial-angular representation (15) of the partial waves help carry out the integration over the angle and spin variables analytically.

To obtain the partial-wave expansion of the many-electron scattering states, we now combine Eqs. (14) and (15) together with the stardard procedure for the coupling of two angular momenta

$$\begin{aligned}|\alpha_i J_i M_{J,i}, \mathbf{p}m_s\rangle &= \mathcal{A}\sum_{\kappa} i^l e^{i\Delta_\kappa}\sqrt{4\pi}[l]^{1/2}\langle l01/2m_s|jm_s\rangle|\epsilon\kappa jm_s\rangle \\ &\quad\times|\alpha J_i M_{J,i}\rangle \\ &= \mathcal{A}\sum_{\kappa,J,M_i} i^l e^{i\Delta_\kappa}\sqrt{4\pi}[l]^{1/2}\langle l01/2m_s|jm_s\rangle \\ &\quad\times\langle J_i M_{J,i} jm_s|JM_i\rangle\times|(\alpha_i J_i,\epsilon lj)JM_i\rangle,\end{aligned} \tag{16}$$

and where the operator $\mathcal{A}$ is used to ensure the proper antisymmetrization of the outgoing electron (coordinate) with respect to all the bound-state orbitals. Combining the three expansions (13), (15), and (16), we therefore see that the transition amplitude (12) can be written as

$$\begin{aligned}&\langle(I,\alpha_i J_i)F_i M_{F,i}, \mathbf{p}m_s|\hat{\mathcal{R}}_\lambda(\mathbf{k})|(I,\alpha_f J_f)F_f M_{F,f}\rangle \\ &\quad= \sum_{M_I,M_{J,i},M_{J,f}}\sum_{\kappa,J,M_i} i^{-l}e^{-i\Delta_\kappa}\sqrt{4\pi}[l]^{1/2}\langle IM_I J_i M_{J,i}|F_i M_{F,i}\rangle \\ &\quad\times\langle IM_I J_f M_{J,f}|F_f M_{F,f}\rangle\langle l01/2m_s|jm_s\rangle\langle J_i M_{J,i} jm_s|JM_i\rangle \\ &\quad\times\langle(\alpha_i J_i,\epsilon lj)JM_i|\hat{\mathcal{R}}_\lambda(\mathbf{k})|\alpha_f J_f M_{J,f}\rangle\end{aligned} \tag{17}$$

and that, for our further discussion of the transition matrix, it is sufficient to consider the matrix element $\langle(\alpha_i J_i,\epsilon lj)JM_i|\hat{\mathcal{R}}_\lambda(\mathbf{k})|\alpha_f J_f M_{J,f}\rangle$ of the electron-photon interaction, taken between the two N-electron states with well-defined total angular momentum and parity.

Equation (17) represents the most general form of the transition matrix for the capture or emission of an electron by ions with a non-zero nuclear spin; at least, al long the operator $\hat{\mathcal{R}}_\lambda(\mathbf{k})$ does not depend on I, and if we neglect the (configuration) interaction between different scattering states in the continuum. We shall return to this form of the transition matrix in some forthcoming contribution where we will study the effects of the ion and/or electron polarization on the photon emission. For the total and angle-differential cross sections, in contrast, we may suppose below—without any further restriction—a zero nuclear spin $I=0$ for which the transition amplitude (17) simplifies to

$$\begin{aligned}&\langle\alpha_i J_i M_{J,i}, \mathbf{p}m_s|\hat{\mathcal{R}}_\lambda(\mathbf{k})|\alpha_f J_f M_{J,f}\rangle \\ &\quad= \sum_{\kappa,J,M_i} i^{-l}e^{-i\Delta_\kappa}\sqrt{4\pi}[l]^{1/2}\langle l01/2m_s|jm_s\rangle\times\langle J_i M_{J,i} jm_s|JM_i\rangle \\ &\quad\times\langle(\alpha_i J_i,\epsilon lj)JM_i|\hat{\mathcal{R}}_\lambda(\mathbf{k})|\alpha_f J_f M_{J,f}\rangle.\end{aligned} \tag{18}$$

D. Electron-photon interaction

Having used the symmetry properties of the many-electron states in the density matrix (17), we only need to discuss the electron-photon interaction in order to obtain an expression, which can finally be calculated. Of course, the interaction of the electrons with the radiation field has been frequently described in the literature as it similarly occurs in atomic photoionization and in the computation of transition probabilities; its operator

$$\hat{\mathcal{R}}_\lambda(\mathbf{k}) = \sum_p \boldsymbol{\alpha}_p\cdot\mathcal{A}_{\lambda,p}(\mathbf{k}) = \sum_p \boldsymbol{\alpha}_p\cdot\mathbf{u}_{\lambda,p}e^{i\mathbf{k}\cdot\mathbf{r}_p} \tag{19}$$

can be written as a sum of one-particle operators, where $\alpha_p = (\alpha_{p,x},\alpha_{p,y},\alpha_{p,z})$ denotes the vector of the Dirac matrices for the pth particle and $\mathcal{A}_{\lambda,p}(\mathbf{k})$ the vector potential of the radiation field. To further simplify the transition matrix (17), of course, the operator $\hat{\mathcal{R}}_\lambda(\mathbf{k})$ must be represented in terms of spherical tensors, i.e., in terms of its electric and magnetic multipole fields. In the helicity representation of the photon ($\mathbf{e}_z\|\mathbf{k}$), the vector potential is given by [19]

$$\begin{aligned}\mathcal{A}_\lambda(\mathbf{e}_z\|\mathbf{k}) &= \sqrt{2\pi}\sum_L i^L[L]^{1/2}(\mathbf{A}_{L\lambda}^{(m)} + i\lambda\mathbf{A}_{L\lambda}^{(e)}) \\ &= \sqrt{2\pi}\sum_L\sum_{\pi=0,1} i^L[L]^{1/2}(i\lambda)^\pi\mathbf{A}_{L\lambda}^{\pi},\end{aligned} \tag{20}$$

where, in the second line, $\pi=0$ refers to the magnetic and $\pi=1$ to the electric multipoles. Since, as mentioned before, it is often more convenient to choose the electron momentum as quantization axis, we need further to rotate the vector potential (20) in space so that its z axis coincides with the electron momentum

$$\mathcal{A}_\lambda(\mathbf{k}) = \sqrt{2\pi}\sum_{L,M}\sum_{\pi=0,1} i^L[L]^{1/2}(i\lambda)^\pi\mathbf{A}_{L\lambda}^{\pi}D_{M\lambda}^{L}(\mathbf{k}\to\mathbf{e}_z). \tag{21}$$

Here, $D_{M\lambda}^{L}(\mathbf{k}\to\mathbf{e}_z)$ is the Wigner rotation matrix of rank L, which has to be applied independently to each irreducible tensor component of the field. The decomposition (20) of the photon field in terms of its irreducible components with well-defined transformation properties enables us to carry out the spin-angular integration analytically by using the techniques from Racah's algebra [20].

Making use of Eqs. (19)–(21) in the transition matrix (18) and by changing the sequence of summation ($LM\pi \leftrightarrow p$), we obtain

$$\begin{aligned}
&\langle \alpha_i J_i M_{J,i}, \mathbf{p}m_s | \hat{\mathcal{R}}_\lambda(\mathbf{k}) | \alpha_f J_f M_{J,f} \rangle \\
&= \left\langle \alpha_i J_i M_{J,i}, \mathbf{p}m_s \left| \sum_p \boldsymbol{\alpha}_p \cdot \mathcal{A}_{\lambda,p}(\mathbf{k}) \right| \alpha_f J_f M_{J,f} \right\rangle \\
&= \sqrt{2\pi} \sum_{L,M,\pi} i^L [L]^{1/2} (i\lambda)^\pi D^L_{M\lambda}(\mathbf{k} \to \mathbf{e}_z) \\
&\quad \times \left\langle \alpha_i J_i M_{J,i}, \mathbf{p}m_s \left| \sum_p \boldsymbol{\alpha}_p \cdot \mathbf{A}^\pi_{LM,p}(\mathbf{k}) \right| \alpha_f J_f M_{J,f} \right\rangle \\
&= 2\pi\sqrt{2} \sum_{L,M,\pi,kJM_i} i^L (i\lambda)^\pi \frac{[L,l]^{1/2}}{[J]^{1/2}} \langle l01/2m_s | jm_s \rangle \\
&\quad \times \langle J_i M_{J,i} jm_s | JM_i \rangle \langle J_f M_{J,f} LM | JM_i \rangle \\
&\quad \times \langle (\alpha_i J_i, \epsilon lj) J \| H_\gamma(\pi L) \| \alpha_f J_f \rangle D^L_{M\lambda}(\mathbf{k} \to \mathbf{e}_z), \qquad (22)
\end{aligned}$$

where, in the last line, we made use of the Wigner-Eckart theorem [15,20] and the notation

$$\begin{aligned}
&\langle (\alpha_i J_i, \epsilon lj) J \| H_\gamma(\pi L) \| \alpha_f J_f \rangle \\
&\quad = i^{-l} e^{-i\Delta_\kappa} \left\langle (\alpha_i J_i, \epsilon lj) J \left\| \sum_p \boldsymbol{\alpha}_p \cdot \mathbf{A}^\pi_{L,p}(\mathbf{k}) \right\| \alpha_f J_f \right\rangle \qquad (23)
\end{aligned}$$

to denote the reduced matrix elements of the multipole fields together with the proper phase for the captured electron. In fact, the reduced matrix elements (23) are the building blocks in order to represent and to discuss a large number of REC properties. An efficient evaluation of these matrix elements is crucial for studying the radiative capture by few— and many—electron ions. Note that by using the reduced form of the transition matrix, the building blocks (23) are independent of the particular choice of the quantization axis.

Equation (22) displays the (REC) transition matrix for the capture or emission of a single electron by a many-electron ion. For the capture into bare ions, we have $J_i = M_{J,i} = 0$ and $(\alpha_f J_f M_{J,f}) = (n_b j_b m_b)$ in order to designate the bound state of the hydrogenlike ion, and hence the transition matrix (22) simplifies to

$$\begin{aligned}
&\langle \mathbf{p}m_s | \hat{\mathcal{R}}_\lambda(\mathbf{k}) | n_b j_b \mu_b \rangle \\
&\quad = 2\pi\sqrt{2} \sum_{\kappa,L,M,\pi} i^{-l+L} e^{-i\Delta_\kappa} (i\lambda)^\pi \frac{[L,l]^{1/2}}{[j]^{1/2}} \langle l01/2m_s | jm_s \rangle \\
&\qquad \times \langle j_b \mu_b LM | jm_s \rangle \langle \epsilon lj \| \boldsymbol{\alpha} \mathbf{A}^\pi_L \| n_b j_b \rangle D^L_{M\lambda}(\mathbf{k} \to \mathbf{e}_z), \quad (24)
\end{aligned}$$

in agreement with the reduced (one-electron) matrix elements as displayed in our previous work [5], Appendix A.

E. Final-state density matrix

The density matrix (4) contains all information about the REC photon and the residual ion after one electron has been captured. Therefore, this representation can be utilized as starting point for describing a large number of processes following the radiative capture of electrons. In this contribution, we make use of Eq. (6) in order to calculate the total cross sections and angular distributions for the capture of electrons by few-electron ions. For the final representation of this matrix, of course, we shall use the multipole expansion of the electron and photon field from Secs. II C and II D. Substituting the transition matrix (22) into Eq. (4), the final-state density matrix is given by

$$\begin{aligned}
\langle \alpha_f J_f M_{J,f}, \mathbf{k}\lambda | \hat{\rho}_f | \alpha_f J_f M'_{J,f}, \mathbf{k}\lambda' \rangle &= \frac{1}{2(2J_i+1)} \sum_{M_{J,i},m_s} \langle \alpha_f J_f M_{J,f} | \hat{\mathcal{R}}^\dagger_\lambda(\mathbf{k}) | \alpha_i J_i M_{J,i}, \mathbf{p}m_s \rangle \langle \alpha_i J_i M_{J,i}, \mathbf{p}m_s | \hat{\mathcal{R}}_{\lambda'}(\mathbf{k}) | \alpha_f J_f M'_{J,f} \rangle \\
&= \frac{8\pi^2}{2(2J_i+1)} \sum_{\pi,L,\pi',L',J,J'} \sum_{\kappa,\kappa'} \sum_{\nu,\mu_1,\mu_2,s,s'} D^\nu_{\mu_2\mu_1}(\mathbf{k} \to \mathbf{e}_z) i^{L'-L} (i\lambda')^{\pi'} (-i\lambda)^\pi \\
&\quad \times (-1)^{1/2+J_i+J'+L+s+s'-M'_{J,f}} [l,l',L,L',j,j',J,J',s]^{1/2} \times [s'] \begin{Bmatrix} j' & 1/2 & l' \\ l & s & j \end{Bmatrix} \begin{Bmatrix} j' & J_i & J' \\ J & s & j \end{Bmatrix} \\
&\quad \times \begin{Bmatrix} J & L & J_f \\ \nu & s' & L' \end{Bmatrix} \begin{Bmatrix} J & J' & s \\ J_f & s' & L' \end{Bmatrix} \langle l'0l0 | s0 \rangle \langle J_f M_{J,f} s' - M'_{J,f} | \nu\mu_1 \rangle \langle s0s' M'_{J,f} | J_f M'_{J,f} \rangle \\
&\quad \times \langle L'\lambda' L - \lambda | \nu\mu_2 \rangle \langle (\alpha_i J_i, \epsilon lj) J \| H_\gamma(\pi L) \| \alpha_f J_f \rangle^* \langle (\alpha_i J_i, \epsilon l' j') J' \| H_\gamma(\pi' L') \| \alpha_f J_f \rangle, \qquad (25)
\end{aligned}$$

if a nuclear spin $I=0$ is supposed, and by using Racah's algebra to eliminate the summation over all the intermediate magnetic quantum numbers. Indeed, this formula is the main result of this work and will be utilized later for studying a number of properties of the emitted photons and residual ions, other than the total or angle-differential cross sections. For instance, it will be applied also in our forthcoming work for stydying the REC emission in dependence on the polarization of the incoming electrons and/or ions, respectively.

The density matrix (25) describes the overall system "ion+photon" following the capture of an electron. If the capture leads to an excited state of the ion and if the REC

photon is not recorded by the experiment, the final-state density matrix of the *ion* is obtained by carrying out the summation over the photon quantum numbers [see. Eq. (9)]

$$\langle \alpha_f J_f M_{J,f} | \hat{\rho}_f^{\rm ion} | \alpha_f J_f M'_{J,f} \rangle = \sum_\lambda \int d\Omega \langle \alpha_f J_f M_{J,f}, \mathbf{k}\lambda | \hat{\rho}_f | \alpha_f J_f M'_{J,f}, \mathbf{k}\lambda \rangle, \quad (26)$$

while the statistical tensors of the residual ions (11) are given by

$$\rho_{k0}(\alpha_f J_f) = \frac{32\pi^3}{2J_i+1} \sum_{L\pi} \sum_{JJ'\kappa\kappa'} [l,l',j,j',J,J']^{1/2} \times (-1)^{J_i+L-J_f+J-J'-1/2} \langle l0l'0|k0\rangle \begin{Bmatrix} j & j' & k \\ l' & l & 1/2 \end{Bmatrix} \times \begin{Bmatrix} j & j' & k \\ J' & J & J_i \end{Bmatrix} \begin{Bmatrix} J & J' & k \\ J_f & J_f & L \end{Bmatrix} \times \langle (\alpha_i J_i, \epsilon l j) J \| H_\gamma(\pi L) \| \alpha_f J_f \rangle \times \langle (\alpha_i J_i, \epsilon l' j') J' \| H_\gamma(\pi L) \| \alpha_f J_f \rangle^*. \quad (27)$$

As seen from this formula, a considerable simplification arises (now) for the statistical tensors owing to their definition as *spherical* tensors [20]. The rank-zero tensor $\rho_{00} \neq \rho_{00}(\theta,\phi)$ has a particular meaning

$$\rho_{00} \propto \frac{1}{\sqrt{2J_f+1}} \sigma_{\rm tot}^{\rm REC} \quad (28)$$

as it represents (up to the factor $1/\sqrt{2J_f+1}$) the total cross section for the capture of an electron into the level $(\alpha_f J_f)$ of the ion and if the density matrix is normalized due to the relation (10). The statistical tensors of higher rank $\rho_{k0}(\theta,\phi)$ with $k>0$, in contrast, are known to refer to the population of the various substates relative to each other and, hence, to represent the orientation and alignment of the ions [15,16].

F. Total cross sections

Using Eq. (27), we obtain the rank-zero statistical tensor

$$\rho_{00}(\alpha_f J_f) = \frac{32\pi^3}{(2J_i+1)\sqrt{2J_f+1}} \sum_{L\pi J\kappa} |\langle (\alpha_i J_i, \epsilon l j) J \| H_\gamma(\pi L) \| \alpha_f J_f \rangle|^2 \quad (29)$$

as the sum over all the (allowed combinations of the) multipoles and capture channels in the one-electron continuum of the ions, and as known from the literature [5,15]. With this scalar, the total cross sections [see Eq. (8)] becomes

$$\sigma_{|J_f\rangle}^{\rm REC} = 8\alpha^3\pi^3 \frac{\omega}{(2J_i+1)} \frac{1}{\beta^2\gamma^2} \times \left[\sum_{L\pi J\kappa} |\langle (\alpha_i J_i, \epsilon l j) J \| H_\gamma(\pi L) \| \alpha_f J_f \rangle|^2 \right] \quad (30)$$

if the density of states and the principle of detailed balance between the capture and the ionization of an electron is taken into account [1]. In Eq. (30), moreover, α denotes the fine-structure constant, while $\beta=v/c$ and $\gamma=\sqrt{1-\beta^2}$ arise from the Lorentz transformation in going from the projectile into the laboratory frame. For the capture by bare (or closed-shell) ions, again, we have $J_i=0$ and $J_f=j_b$, i.e., the angular momentum of the (bound) single valence electron, from which we obtain the total cross section

$$\sigma_{j_b}^{\rm REC} = 8\alpha^3\pi^3 \frac{\omega}{\beta^2\gamma^2} \left[\sum_{L\pi\kappa} |\langle \epsilon l j \| H_\gamma(\pi L) \| n_b j_b \rangle|^2 \right], \quad (31)$$

as shown and calculated before at various places in the literature [1,8,21].

G. Angular distribution of the recombination photons

As discussed in Sec. II B, the angular distribution of the emitted REC photons is obtained from the final-state density matrix by taking $\mathrm{Tr}(\hat{P}_{\mathbf{k}}\hat{\rho}_f)$, i.e., the trace over the product of the projection operator (5) and the density matrix (25),

$$W(\theta) = \frac{\sigma_{|J_f\rangle}^{\rm REC}}{4\pi} \left(1 + \sum_{\nu=1} P_\nu(\cos\theta) \beta_\nu^{\rm REC}(\alpha_i J_i, \alpha_f J_f) \right), \quad (32)$$

and where the anisotropy coefficients are given by

$$\beta_\nu^{\rm REC} = -\frac{1}{2} \sum_{JJ'\kappa\kappa'} \sum_{L\pi L'\pi'} i^{L+\pi-L'-\pi'} (-1)^{J_i-1/2-J_f} \times [L,L',l,l',j,j',J,J']^{1/2} \langle l0l'0|\nu0\rangle \langle L1L'-1|\nu0\rangle \times (1+(-1)^{L+\pi+L'+\pi'-\nu}) \begin{Bmatrix} J & J' & \nu \\ L' & L & J_f \end{Bmatrix} \times \begin{Bmatrix} J & J' & \nu \\ j' & j & J_i \end{Bmatrix} \begin{Bmatrix} j & j' & \nu \\ l' & l & 1/2 \end{Bmatrix} \times \langle \alpha_i J_i, \epsilon l j : J \| H_\gamma(\pi L) \| \alpha_f J_f \rangle \times \langle \alpha_i J_i, \epsilon l' j' : J' \| H_\gamma(\pi' L') \| \alpha_f J_f \rangle^* \times \left[\sum_{L\pi J\kappa} |\langle \alpha_i J_i, \epsilon l j : J \| H_\gamma(\pi L) \| \alpha_f J_f \rangle|^2 \right]^{-1}. \quad (33)$$

As seen from this and formula (30), the reduced matrix elements (23) are again the central entities in calculating the total cross sections and angular distributions; for the capture into bare ions, it simplifies to

$$\beta_\nu^{\rm REC,bare} = -\frac{1}{2} \sum_{\kappa\kappa'} \sum_{L\pi L'\pi'} i^{L+\pi-L'-\pi'} (-1)^{j+j'-1/2-j_b+\nu} \times [L,L',l,l',j,j']^{1/2} \times \langle l0l'0|\nu0\rangle \langle L1L'-1|\nu0\rangle [1 + (-1)^{L+\pi+L'+\pi'-\nu}] \begin{Bmatrix} j & j' & \nu \\ L' & L & j_b \end{Bmatrix} \begin{Bmatrix} j & j' & \nu \\ l' & l & 1/2 \end{Bmatrix} \times \langle \epsilon l j \| H_\gamma(\pi L) \| n_b j_b \rangle \langle \epsilon l' j' \| H_\gamma(\pi' L') \| n_b j_b \rangle^* \times \left[\sum_{L\pi\kappa} |\langle \epsilon l j \| H_\gamma(\pi L) \| n_b j_b \rangle|^2 \right]^{-1}. \quad (34)$$

Equations (30) and (32) represent the most general form of the total REC cross sections and the angular distribution of the emitted photons, as long as the hyperfine interaction be-

tween the magnetic moments of the electrons and ions is neglected. They can be used for any shell structure of the atoms and ions (although, of course, difficulties might arise in generating the corresponding wave functions). Since the hyperfine interaction is suppressed by about 5–6 orders of magnitude, when compared to the interaction of the electrons with the radiation field, this approximation is well justified for all practical purposes. Below, we make use of these equations to explore the REC into hydrogenlike U^{91+} ions, leading to a heliumlike $1s^2\ ^1S_0$ ground state, as well as the capture into the $1s^2\,2lj$ (excited) states of the lithiumlike U^{89+} ions.

III. COMPUTATIONS

As seen from the formalism above, the computation of (most) REC properties can be traced back to the reduced matrix element (23), which describes the interaction of an ionic bound state with the one-electron continuum due to the presence of the radiation field. Apart from the boundary conditions, which are specific to the radiative recombination, not much needs to be said here about the further evaluation of these reduced matrix elements as they frequently occur in the computation of atomic properties, such as transition probabilities and photoionization cross sections, and have thus been implemented in quite a number of approximations. In our computations below, the multiconfiguration Dirac-Fock (MCDF) method is used to generate the ionic bound-state wave functions and to evaluate all the required matrix elements.

In the past years, the MCDF method was found useful for studying multiple and highly charged ions, especially if innershell electrons or several open shells are involved in the computations [22,23]. In this method, an atomic state is approximated by a linear combination of (so-called) configuration state functions (CSFs) of the same symmetry

$$\psi_\alpha(PJM) = \sum_{r=1}^{n_c} c_r(\alpha)\,|\gamma_r PJM\rangle, \tag{35}$$

where n_c is the number of CSF and $\{c_r(\alpha)\}$ denotes the representation of the atomic state in this basis. In most standard computations, the CSF are constructed as antisymmetrized products of a common set of orthonormal orbitals and are optimized on the basis of the Dirac-Coulomb Hamiltonian. Further relativistic contributions to the representation $\{c_r(\alpha)\}$ of the atomic states are then added, owing to the given requirements, by diagonalizing the Dirac-Coulomb-Breit Hamiltonian matrix in first-order perturbation theory. For multiple and highly charged ions, moreover, an estimate of the dominant QED contributions (i.e., the self-energy and vacuum polarization of the electronic cloud) can be taken into account also by using data from the hydrogenlike ions and a proper scaling of the charge distribution near and around the nucleus. In order to support a reliable estimate of the REC amplitudes, a new component (REC) has been developed recently within the framework of the RATIP package [24], which now facilitates the computation of the cross sections and angular distrubutions within a distorted-wave approximation.

Despite the similarities in the setup of the REC program with a corresponding component for atomic photoionization [24], there are a number of differences in studying the REC by highly charged ions, which should be taken into account. Since we consider here the capture by fast high-Z ions, a sufficiently large number of partial waves has to be incorporated into the expansion of the electron and photon fields, quite in difference to atomic photoionization where one rarely goes beyond the *electric-dipole* approximation. For the REC into high-Z ions, in contrast, several ten or even hundred capture channels need to be included due to the allowed combinations of the partial electron waves κ and the multipoles (πL) of the radiation field. For the capture into the $1s^2\ ^1S_0$ ground state of 120 MeV/u uranium, i.e., initially hydrogenlike U^{91+} ions for example, we had to include all partial waves with $|\kappa| \leqslant 15$ in order to obtain a smoothly converged distribution for all angles $0 \leqslant \theta \leqslant \pi$.

IV. RESULTS AND DISCUSSIONS

The capture into high-Z few-electron ions offers a unique possibility for studying the interplay between the electron-photon and electron-electron interaction in the presence of strong fields. It also enables one to explore the coupling of deeply bound electrons to the continuum. For the REC into few-electron ions, therefore, the major interest perhaps concerns the capture into hydrogenlike and lithiumlike ions (as the simplest many-electron systems), where the fine structure of the ions in their final state may influence the cross sections and angular distribution of the emitted photons. Below we consider especially the capture into U^{91+} and U^{89+} uranium ions as function of the projectile energy, and discuss the corresponding angular distributions.

A. Capture into hydrogenlike ions

If an electron is captured by hydrogenlike projectiles, we find the ions either in the $1s^2\ ^1S_0$ ground state or in one of the $1s\,nlj\ ^{1,3}L_J$ excited states of the heliumlike system. These states differ from the capture into bare ions, in particular, by the coupling of the (electron) angular momenta, while only a rather small effect is expected from the screening of the nuclear charge owing to the additional K-shell electron. For high-Z ions, such as hydrogenlike U^{91+}, we therefore expect a minor influence on the total and angle-differential cross sections if the capture into the $1s^2\ ^1S_0$ ground configuration is considered [apart from the factor 1/2 which arises from the (pre) occupation of the K shell]. In Table I, we display the total K-shell cross sections for three different projectile energies and compare the results from the MCDF computations with those as obtained for bare ions, using an (effective) charge Z_{eff}=92. In the MCDF approximation, moreover, all the cross sections have been calculated witin two different gauges for the coupling of the radiation field, namely the Babushkin and Coulomb gauge, which—in the nonrelativistic limit—correspond to the length and velocity gauge, respectively. Although an agreement of the various gauges does not prove the correctness of any result, the differences between the length and velocity gauge are often

TABLE I. Total cross sections (in b) for the radiative electron capture into the $1s^2\ ^1S_0$ ground state of (initially) hydrogenlike uranium ions U^{91+} in dependence of the projectile energy T_p. The cross sections have been calculated within an effective one-particle model with charge $Z_{\text{eff}}=92$ as well as within the MCDF approximation by applying two different gauges for the coupling of the radiation field. See text for further details.

	T_p (MeV/u)		
	2.18	21.8	218
Bare ion ($Z_{\text{eff}}=92$)	7.258×10^3	6.898×10^2	4.617×10^1
MCDF (Coulomb gauge)	7.058×10^3	6.824×10^2	4.569×10^1
MCDF (Babushkin gauge)	7.175×10^3	6.714×10^2	4.538×10^1

taken as an indication for the accuracy of many-electron computations.

As seen from Table I, the total K-shell cross sections differ by less or approximately 2%, if calculated within the (many-electron) MCDF method or simply by using an effective one-particle model, and by taking the initial occupation of the K shell into account. For the capture into the $1s^2\ ^1S_0$ ground state, these small differences appear (almost) independent from the projectile energy down to $T_p=2.18$ MeV/u. No many-electron effects are seen also in the angular distribution of the K-REC photons, independent of the projectile energy, as shown in Fig. 2 for the three energies $T_p=2.18$, 21.8, and 218 MeV/u, respectively. While projectile energies $T_p \gtrsim 100$ MeV/u are presently already available for high-Z ions, for instance, at the GSI in Darmstadt, the further decelleration of the ion beams is one of the prospects of the new GSI facility, which is planned to be extended during the next decade. Slow ion beams with less than a few MeV/u are of interest, in particular, for studying electron-electron interaction effects in strong fields as the correlation energy has to be compared to the kinetic energy of the (projectile) electrons in the beam.

For the capture into the K shell, the agreement between the MCDF computation and the effective one-particle approximation above can be understood easily by comparing the kinetic and the binding energies of the electrons in the

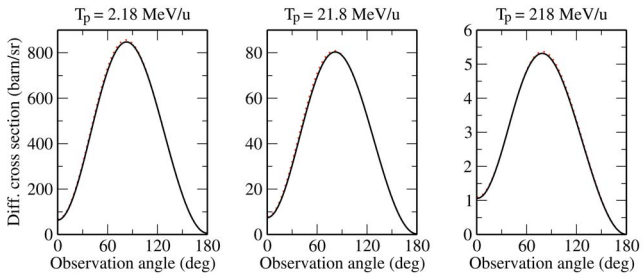

FIG. 2. (Color online) Angle-differential cross sections for the radiative electron capture into the $1s^2\ ^1S_0$ ground state of (initially) hydrogenlike uranium ions U^{91+} with projectile energies $T_p=2.18$, 21.8, and 218 MeV/u. Results are presented for an effective one-particle model with $Z_{\text{eff}}=92$ (– – –) and for the MCDF method (—) using Babushkin gauge.

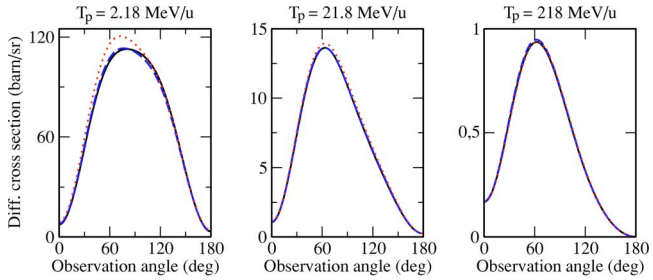

FIG. 3. (Color online) Angle-differential cross sections for the radiative electron capture into the $1s^2\ 2s^2$ state of (initially) lithiumlike uranium ions U^{89+} with projectile energies of 2.18, 21.8, and 218 MeV/u. Results from an independent particle model with an effective charge $Z_{\text{eff}}=91$. (– – –) are compared with those from MCDF calculations in Coulomb (—) and Babushkin gauge (– –).

REC process. Although, for a beam energy of 2.18 MeV/u, the (quasi) free electrons in either the target atoms or the electron cooler have a kinetic energy of only T_e [keV]$=1.2\approx T_p$ [MeV/u]/1.8, the large $1s$ binding energy of about 130 keV for hydrogenlike U^{91+} ions ensures, that the K-shell capture is well described within a one-particle model, in good agreement with earlier observations [13]. A slightly larger effect could be expected for the capture into the L shell, i.e., the $1s2lj\ ^{1,3}S$ and $^{1,3}P$ states of (finally) heliumlike uranium, even though this would require then the resolution of the various fine-structure levels in the REC spectra (which has not been achieved so far). Electron-electron interaction effects have become visible also if the subsequent $K\alpha$ characteristic photon emission is observed [25]. A more detailed analysis of this subsequent decay from the $1s2lj\ ^{1,3}L_L$ levels, following the L-shell REC into hydrogenlike uranium requires, however, to describe the alignment of the excited and will be the subject of our forthcoming work.

B. Capture into lithiumlike ions

For lithiumlike ions initially, the capture into the L shell leads to the $1s^2\ 2s\ 2lj\ ^{1,3}L_J$ levels including the $1s^2\ 2s^2\ ^1S_0$ ground state of the berylliumlike ions. For the L shell, or course, the binding energy of the captured electron is about four times smaller than for the K shell, so that many-electron effects on the total and angle-differential cross sections of the emitted L-REC photons may be hereby observed easier. For the total cross sections, in fact, a proper screening of the nuclear charge due to the three electrons in the $1s^2\ 2s\ ^2S_{1/2}$ lithiumlike ground state must be taken into account.

Figure 3 displays the angle-differential cross sections for the L-shell capture into the $1s^2\ 2s^2$ state of (initially) lithiumlike U^{89+} ions, and calculated for the same projectile energies of 2.18, 21.8, and 218 MeV/u as applied above for the capture into the K shell. Results from the MCDF calculation in Coulomb and Babushkin gauge are compared to the data from an independent-particle approximation (using Slater determinants with hydrogenlike, one-electron orbitals) with an effective charge $Z_{\text{eff}}=91$. This charge was chosen in a way in order to ensure agreement with the MCDF calculations for high projectile energies. A similar scaling of one-electron

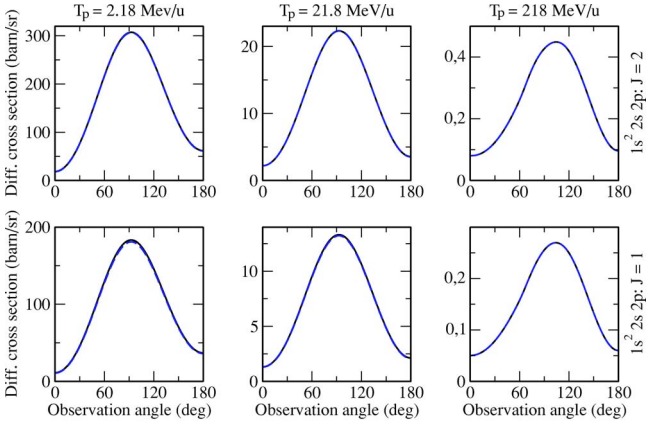

FIG. 4. (Color online) Angle-differential cross sections for the radiative electron capture into the $1s^2\,2s\,2p_{3/2}$ states of (initially) lithiumlike uranium ions U^{89+} with projectile energies of 2.18, 21.8, and 218 MeV/u. Results from MCDF calculations are shown in Coulomb (—) and Babushkin gauge (– –).

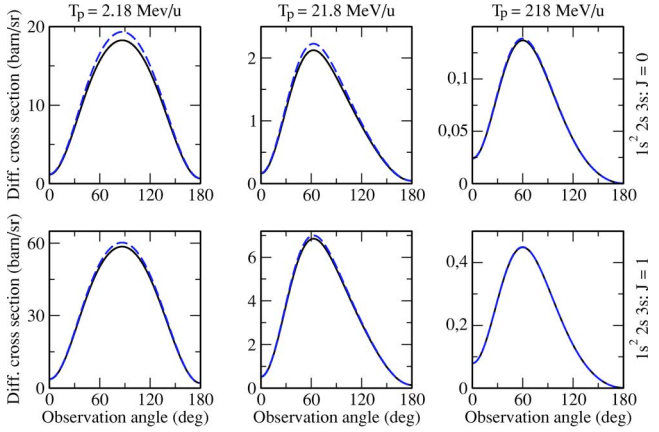

FIG. 5. (Color online) Angle-differential cross sections for the radiative electron capture into the $1s^2\,2s\,3s$ states of (initially) lithiumlike uranium ions U^{89+} with projectile energies of 2.18, 21.8, and 218 MeV/u. Results from MCDF calculations are shown in Coulomb (—) and Babushkin gauge (– –).

results was applied before by Bednarz *et al.* [13] for comparison with an experimentally observed angular distribution of the L-shell REC photons for lithiumlike uranium, however, without information about the effective charge which was taken at that time. In Fig. 3, note the excellent agreement of the two gauge forms within about the thickness of the curves. For medium and large projectile energies of, say, $T_p \gtrsim 100$ MeV/u or $T_e \gtrsim 50$ keV electron energy, respectively, there are virtually no differences between the many-electron treatment and the use of the independent-particle model. A small deviation between these two theories only arise at small projectile energies of 2.18 MeV/u, for which the decrease (and shift) in the angular distribution near $\theta \approx 60°$ indicate electron-electron correlation effects upon the radiative electron capture. Even larger effects are to be expected if the projectiles are further decelerated towards a zero kinetic energy as it might be realized at electron-beam ion traps (EBIT) or the future GSI facility [26].

The capture into the $1s^2\,2s^2$ ground configuration of the beryllium sequence leads to a closed-shell $^1S_0$ state which can well be approximated by a single Slater determinant. For the capture of the electron into the $2p_{1/2}$ and $2p_{3/2}$ subshells, in contrast, at least the coupling of the (one-electron) angular momenta has to be taken into account in addition to the antisymmetrization of the wave functions due to Pauli's principle. In Fig. 4, we display the angular distributions for the capture into the (upper) $1s^2\,2s\,2p_{3/2}$ $J=1,2$ levels which are associated with the (subsequent) $K\alpha_1$ decay. Apart from the total cross sections, which fulfill the statistical ratio 3:5, the angular distributions are rather similar for the $J=1$ and $J=2$ levels, showing a clear enhancement of the angle-differential cross sections in forward direction ($\theta=0°$) as the projectile energy is increased. For the capture into these excited states, there occurs also a small deviation between the two gauges which indicate the wave functions for these states to be slightly less accurate than for the representation of the ground states. However, this deviation of $\lesssim 1\%$ is well below of the accuracy which has been achieved so far by any experiment. The gauge dependence of the cross sections is enhanced further for the capture into the M_1 subshell (Fig. 5) where the two $1s^2\,2s\,3s\ ^{1,3}S$ fine-structure levels cannot decay (by dipole-allowed transitions) directly to the ground state. In the experiments, the capture into the $2s\,2p_{3/2}$ $J=1,2$ and $2s\,3s$ $J=0,1$ levels is hardly resolved and, therefore, has often to be treated together.

V. SUMMARY

The density matrix formalism has been applied to describe the radiative electron capture into high-Z, few-electron ions. Based on Dirac's equation, we here developed the theory and notation in order to analyze both, the properties of the photons such as their angular distribution and polarization as well as the level population and decay of the remaining ions. In addition to the present focus on the total and angle-differential REC cross sections, therefore, the formalism is appropriate also for studying the subsequent decay of the ions or the photon-photon angular correlations (whenever possible).

Detailed cross section calculations have been carried out for the capture into hydrogenlike and lithiumlike uranium. These computations confirm (first of all) that an effective one-particle approximation is often sufficient in order to describe the capture by *fast* projectiles, at least if the detectors are not sensitive to the polarization of the REC radiation. However, many-electron effects arise for low projectile energies of $T_p \lesssim 10$ MeV/u, though they are presently not available for high-Z ions. From the study of the angular distribution alone, therefore, not much will be learned at present-day storage rings about the effects of the electron-electron interaction on the REC process; a conclusion, however, which changes radically if the subsequent $K\alpha$ decay or the polarization of the emitted REC photons is considered. While the total cross sections into the ground states can usually be well described within an effective one-particle approximation, moreover, care has to be taken for the capture into the excited states.

In Sec. II, the theoretical treatment of the REC process is independent from the particular shell structure of the ions in their initial and final state. Using the concept of the density matrix, our formalism allows to combine the (long standing) experience in the description of ionic bound states, i.e., the atomic structure part, with those for the electron-photon interaction and for the coupling of bound states to the continuum. It also helps combine the various computer codes which have been developed earlier. Various measurements have been carried out recently, which can be analyzed by means of this formalism, including the angular distribution of the subsequent $K\alpha$ radiation. Other topics of interests concern, for examples, studies on the polarization of the emitted x-ray photons as well as on the polarization effects of either the ion-beam or target atoms. In a forthcoming contribution, we plan to use the formalism above to the capture into the $1s\,2p_{1/2}$ and $1s\,2p_{3/2}$ $^{1,3}P_J$ levels of (initially) hydrogenlike ions and their subsequent $K\alpha_1$ and $K\alpha_2$ decay, which has been observed recently at GSI in Darmstadt and which was found quite in contrast to expectations from a one-particle model.

ACKNOWLEDGMENTS

This work has been supported by the BMBF and the GSI under Project No. KS-FRT.

[1] J. Eichler and W. E. Meyerhof, *Relativistic Atomic Collisions* (Academic Press, San Diego, 1995).
[2] Th. Stöhlker, C. Kozhuharov, P. H. Mokler, A. Warczak, F. Bosch, H. Geissel, R. Moshammer, C. Sheidenberger, J. Eichler, A. Ichihara, T. Shirai, Z. Stachura, and P. Rymuza, Phys. Rev. A **51**, 2098 (1995).
[3] Th. Stöhlker, Phys. Scr. **T80**, 165 (1999).
[4] Th. Stöhlker, D. Banas, S. Fritzsche, A. Gumberidze, C. Kozhuharov, X. Ma, A. Orsic-Muthig, U. Spillmann, D. Sierpowski, A. Surzhykov, S. Tachenov, and A. Warczak, Phys. Scr. **T110**, 384 (2004).
[5] A. Surzhykov, S. Fritzsche, and Th. Stöhlker, J. Phys. B **35**, 3713 (2002).
[6] A. Surzhykov, S. Fritzsche, A. Gumberidze, and Th. Stöhlker, Phys. Rev. Lett. **88**, 153001 (2002).
[7] A. Surzhykov, S. Fritzsche, Th. Stöhlker, and S. Tachenov, Phys. Rev. A **68**, 022710 (2003).
[8] A. Surzhykov, S. Fritzsche, and Th. Stöhlker, Phys. Lett. A **289**, 213 (2001).
[9] J. Eichler and A. Ichihara, Phys. Rev. A **65**, 052716 (2002).
[10] A. Surzhykov, S. Fritzsche, and Th. Stöhlker, Hyperfine Interact. **146–147**, 35 (2003).
[11] J. H. Scofield, Phys. Rev. A **40**, 3054 (1989).
[12] Th. Stöhlker, H. Geissel, H. Irnich, T. Kandler, C. Kozhuharov, P. H. Mokler, G. Münzenberg, F. Nickel, C. Scheidenberger, T. Suzuki, M. Kucharski, A. Warczak, P. Rymuza, Z. Stachura, A. Kriessbach, D. Dauvergne, B. R. Dunford, J. Eichler, A. Ichihara, and T. Shirai, Phys. Rev. Lett. **73**, 3520 (1994).
[13] G. Bednarz, A. Warczak, D. Sierpowski, Th. Stöhlker, S. Hagmann, F. Bosch, A. Gumberidze, C. Kozhuharov, D. Liesen, P. H. Mokler, X. Ma, and Z. Stachura, Hyperfine Interact. **146/147**, 29 (2003).
[14] V. A. Yerokhin, V. M. Shabaev, T. Beier, and J. Eichler, Phys. Rev. A **62**, 042712 (2000).
[15] V. V. Balashov, A. N. Grum-Grzhimailo, and N. M. Kabachnik, *Polarization and Correlation Phenomena in Atomic Collisions* (Kluwer Academic Plenum, New York, 2000).
[16] K. Blum, *Density Matrix Theory and Applications* (Plenum, New York, 1981).
[17] Because of the choice of the transition operator in relation (3), in fact, we evaluate the transition matrix for the "photoionization" of the ion, i.e., for the time-reversed process to the REC.
[18] V. B. Berestetskii, E. M. Lifshitz, and L. P. Pitaevskii, *Relativistic Quantum Theory* (Pergamon, Oxford, 1971).
[19] M. Rose, *Elementary Theory of Angular Momentum* (Wiley, New York, 1957).
[20] U. Fano, and G. Racah, *Irreducible Tensorial Sets* (Academic Press, New York, 1959).
[21] A. Ichihara, T. Shirai, and J. Eichler, Phys. Rev. A **49**, 1875 (1994).
[22] I. P. Grant, in *Methods in Computational Chemistry*, edited by S. Wilson (Plenum Press, New York, 1988), Vol. 2, p. 1.
[23] S. Fritzsche, Phys. Scr. **T100**, 37 (2002).
[24] S. Fritzsche, J. Electron Spectrosc. Relat. Phenom. **114–16**, 1155 (2001).
[25] X. Ma, P. H. Mokler, F. Bosch, A. Gumberidze, C. Kozhuharov, D. Liesen, D. Sierpowski, Z. Stachura, Th. Stöhlker, and A. Warczak, Phys. Rev. A **68**, 042712 (2003).
[26] Conceptual Design Report: An international accelerator facility for beams of ions and antiprotons, GSI (2001).